21st Australasian Fluid Mechanics Conference
Adelaide, Australia
10-13 December 2018

Cooling System design and Performance Analysis for a Supercritical CO_2 Recompression Cycle

M. Monjurul Ehsan, Sam Duniam, Andrew Lock, Yuchen Dai, Zhiqiang Guan, A.Y. Klimenko, H. Gurgenci

School of Mechanical and Mining Engineering
The University of Queensland, Brisbane, QLD 4072, Australia.

Abstract

In the present article, a natural draft dry cooling tower (NDDCT) is designed for a 25 MW recompression sCO_2 Brayton cycle. The thermodynamic property variation with bulk temperature is well predicted by adapting an iterative nodal approach in the heat exchanger. The local property variations of sCO_2 with bulk temperature are taken into consideration since the traditional method of heat exchanger fails to address the heat transfer mechanism, especially for supercritical fluids. The number of finned tube heat exchanger bundles and the tower dimensions (tower height, tower diameter and a number of tower supports) is evaluated to meet the duty requirements. The thermal efficiency of the recompression cycle is validated against various dataset available from the literature. Initially, the thermal assessment of the recompression cycle is carried out in order to obtain the optimum operating conditions (cycle pressure ratio and pre-cooler inlet temperature) for which the cooling tower is designed. Finally, the performance of the cooling tower is investigated for a range of pre-cooler inlet condition (70^0C to 110^0C) and ambient temperature (15^0C to 50^0C). Both the sCO_2 inlet temperature and air temperature significantly influence the cooling performance. During high ambient temperature period, both the cycle efficiency and the heat rejection from the NDDCT decreases.

Introduction

Since the sCO_2 power cycles are mostly suited for concentrated solar power application (CSP) in arid areas, the dry cooling system is receiving much attention in order to reduce the overall cost of the power plant. For commercial-scale power production, the dry cooling unit is an alternative solution due to the scarce water supply and increased power consumption by the mechanical fans in the wet coolers.

Dostal et al. [1] performed the thermal assessment of sCO_2 recompression cycle against helium Brayton cycle. Recompression cycle operating with 550^0C turbine inlet temperature provided equivalent thermal efficiency comparing with helium cycle working at 850^0C. Besarati and Goswami [2] performed modelling of various layouts of sCO_2 cycles (simple cycle, recompression cycle, and partial cooling cycle) integrated with the dry cooling unit for CSP application and recompression cycle attained an efficiency of 50% even with dry cooling. Turchi et al. [3] worked with various configurations of sCO_2 Brayton cycles with intercooling and reheating to achieve higher cycle efficiency at dry climate condition. Conboy et al. [4] reported 43% thermal efficiency with 550^0C turbine inlet temperature and 55^0C compressor inlet temperature with recompression cycle integrated with air-cooled heat exchanger unit. Padilla et al. [5] performed the exergetic analysis of various layouts of sCO_2 cycles integrated with a dry air cooler. The authors also performed the optimization of the recompression cycle with the inclusion of the influence of pressure drop on the cycle performance [6]. Hoo et al. [7] investigated the economic analysis with A-frame finned tube air cooler integrated with sCO_2 Brayton cycles. Osorio et al. [8] performed the dynamic behavior of sCO_2 power cycle at various seasonal conditions and air-cooled heat exchanger was proposed as the cooling component. Li et al. [9] experimented with the trans-critical CO_2 cycle for small-scale power production and air-cooled condenser was used.

Ehsan et al. [10] reported a comprehensive review of heat transfer and pressure drop characteristics of sCO_2 and heat transfer correlations applicable for horizontal tube geometries. The heat transfer mechanism of sCO_2 near the critical condition was investigated under various operating condition. Ehsan et al. [11] developed a validated MATLAB code to design the NDDCT for a 25 MW power plant in CSP application. Later on, the authors analyzed the cooling performance of NDDCT for direct and indirect configuration of the cooling system [12]. The rapid property changes of sCO_2 with a small change of bulk temperature inside the tubes of the air-cooled heat exchanger unit were well predicted by the proposed code. However, these studies were performed without considering the influence of other power cycle components. Most of the research studies focussed on the improvement of thermal efficiency with various configurations of sCO_2 Brayton cycles for CSP application. Few studies focussed on the dry cooling option for power conversion. In these studies, dry cooling was assumed by means of air-cooled heat exchanger unit. Therefore, the scope of the present article is to design a dry cooling system for 25 MW solar power plant. The nodal approach is employed in predicting the heat transfer mechanism and fluid flow behavior in the finned tube heat exchanger bundles. The required tower dimensions and the number of heat exchanger bundles are determined for 25 MW power plant.

Cycle Modelling

In the present work, the dry cooling system is designed for the recompression cycle layout, shown in figure 1. The commercial system simulation software IPSEpro is used to model the power cycle. In the recompression cycle, two recuperators (high-temperature recuperator, HTR and low-temperature recuperator, LTR) are used to recover the heat from the turbine exhaust. After LTR, the flow splitter is used to guide one flow path towards the cooling by NDDCT and another path to the compression process the recompression compressor (RC). The split ratio (SR), significantly influences the cycle performance. The cooled sCO_2 after flowing through the air-cooled heat exchanger bundles is then compressed by the main compressor, MC. The detailed analysis of NDDCT is carried out by the model development kit (MDK) provided by IPSEpro. The thermodynamic property changes with bulk temperature are evaluated by the REFPROP software. All the components work under steady-state operation and minimum pinch point temperature of 5^0C is assumed in the heat exchangers. The heat energy added in the heat source component is a variable to ensure a fixed turbine inlet temperature of 650^0C.

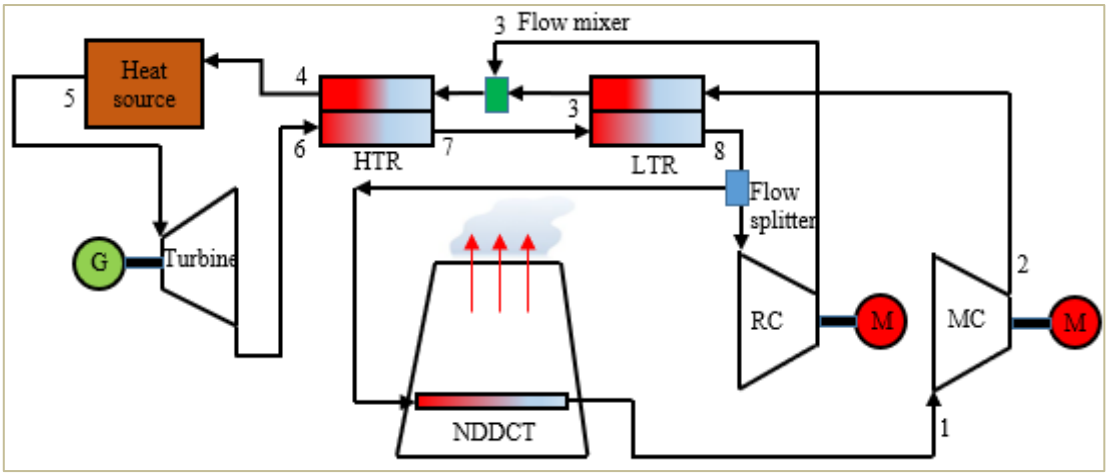

Figure 1. sCO_2 recompression cycle integrated with NDDDCT.

All the turbo-machineries are modelled by defining the isentropic efficiency (0.9 for turbine and 0.89 for all the compressors). The counter-flow arrangement is assumed in the recuperators with a fixed pressure drop of 20 kPa. The heat loss to the surroundings is assumed to be negligible, except for NDDCT. The ambient condition is set at 20^0C with 60% relative humidity and wind velocity of 1 m/s.

Model Validation

For model validation, results are compared with data available from the literature. The cycle thermal efficiency at various turbine inlet temperatures for recompression sCO_2 Brayton cycle is shown in figure 2. The model shows reasonable agreement, although a minor growth in thermal efficiency is observed at higher turbine inlet temperature. This is due to the assumption made in the present analysis. Dostal et al. [1], Turchi et al. [3] and Besarati and Goswami [2] modelled the recuperators by defining the heat exchanger effectiveness, whereas, in the present study, the minimum temperature difference in the LTR is fixed.

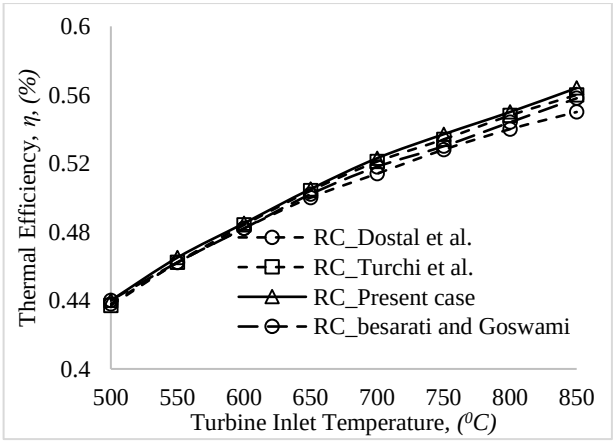

Figure 2. Model validation against literature.

Preliminary Analysis

The effect of compressor inlet temperature on the cycle thermal efficiency and the split ratio is investigated for a fixed turbine inlet pressure and temperature of 20 MPa and 650^0C respectively. For each operating pressure, the efficiency curve shows a peak value near to its respective pseudocritical temperature (35^0C for 8MPa, 40^0C for 9MPa and 45^0C for 10MPa), shown in figure 3. At higher compressor inlet temperature, it is beneficial to increase cycle lower pressure to attain equivalent cycle efficiency. Besarati and Goswami [2] also confirmed the change of trend of the cycle efficiency at higher compressor inlet temperature.

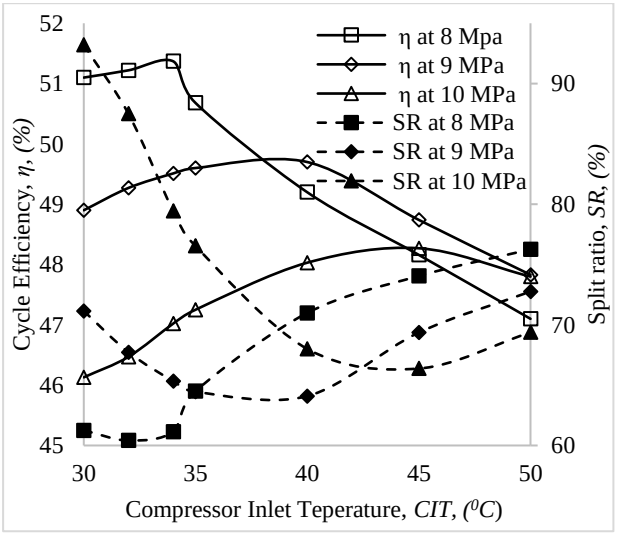

Figure 3. Influence of cycle lower pressure.

Similarly, the effect of cycle higher pressure on thermal efficiency at various compressor inlet temperature is reported in figure 4 for a fixed cycle lower pressure of 8 MPa. The higher the pressure, the greater the cycle thermal efficiency. Likewise, figure 3, the trend of the curve changes at higher compressor inlet temperature. At 35^0C, the efficiency improvement is only about 0.24% and 0.4% for 22 MPa and 24 MPa respectively over the 20 MPa pressure. In the present analysis, cycle higher pressure and lower pressure are kept at 20 MPa and 8 MPa respectively. The variation of *SR* at different cycle lower pressures is also demonstrated. For each operating pressure, the *SR* is minimum at the respective pseudocritical temperature. For each case, the *SR* fairly increases once the pseudocritical region is crossed. The variation of compressor outlet temperature, network-done, W_{net} and heat rejection at different compressor inlet temperature is demonstrated in figure 5 operating at cycle higher pressure of 20 MPa and lower pressure of 8 MPa. The heat rejection by the cycle, Q_{cooler} initially decreases with the compressor inlet temperature. From 35^0C onwards, the heat rejection merely increases. Increasing the compressor inlet temperature increases the compressor outlet temperature and decreases the net-work by the cycle. In figure 6, the variation of split ratio, *SR* and efficiency is plotted against the compressor inlet temperature. The efficiency is maximum about 34^0C and the split ratio also changes in order to maintain the pinch point temperature constriction set at the LTR. The split ratio is minimum at 34^0C at which the cycle thermal efficiency is maximum. From 34^0C onwards, the split ratio linearly increases with the increase of compressor inlet temperature.

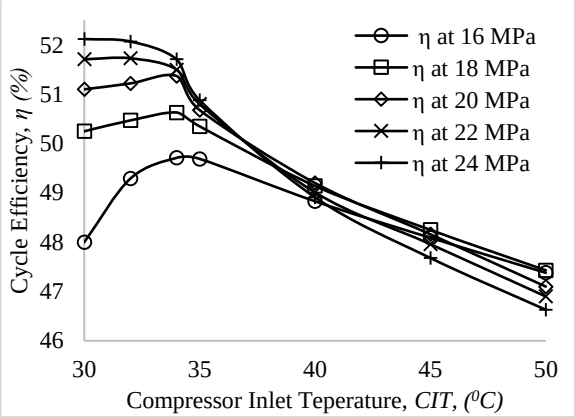

Figure 4. Influence of cycle higher pressure.

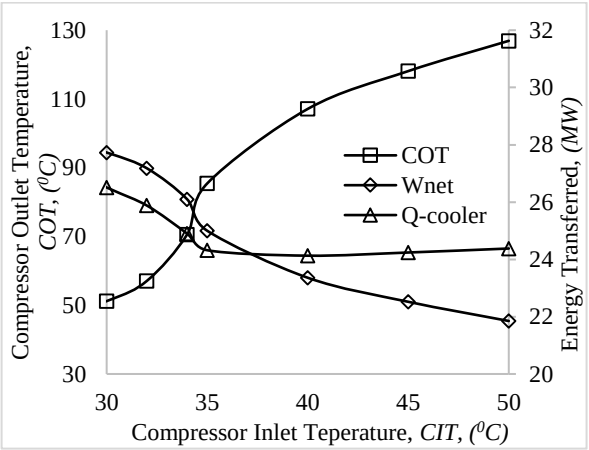

Figure 5. Change of COT, $W_{net,}$ and Q_{cooler} with respect to CIT.

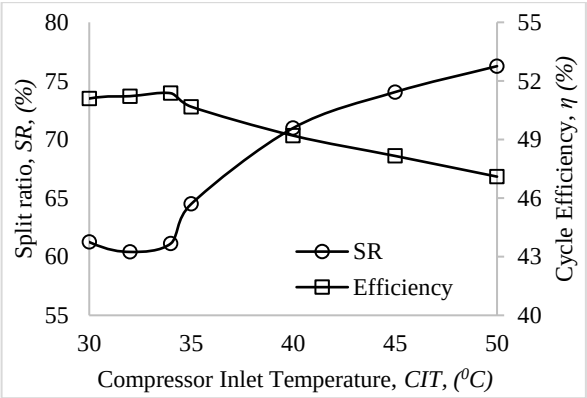

Figure 6. Change of SR and η with respect to CIT.

NDDCT Modelling

In NDDCT, fresh air flows through the bundles of air-cooled heat exchanger unit by means of buoyancy effect. The air has to experience various types of flow resistance while flowing inside the tower. The air mass flow from the tower is determined form the draft equation. The tower support loss efficient K_{ts} is given by

$$K_{ts} = \frac{C_{Dts} L_{ts} d_{ts} n_{ts} A_{fr}^2}{(\pi d_3 H_3)^3} \left(\frac{\rho_{a34}}{\rho_{a1}}\right) \quad (1)$$

Contraction loss efficient, K_{ctc}

$$K_{ctc} = \left(1 - \frac{2}{\sigma_c} + \frac{1}{\sigma_c^2}\right)\left(\frac{\rho_{a34}}{\rho_{a1}}\right)\left(\frac{A_{fr}}{A_{e3}}\right)^2 \quad (2)$$

Expansion loss efficient, K_{cte}

$$K_{cte} = \left(1 - \frac{A_{e3}}{A_3}\right)^2 \left(\frac{\rho_{a34}}{\rho_{a1}}\right)\left(\frac{A_{fr}}{A_{e3}}\right)^2 \quad (3)$$

Cooling tower inlet loss coefficient, K_{ct}

$$K_{ct} = 0.072\left(\frac{d_3}{H_3}\right)^2 - 0.34\left(\frac{d_3}{H_3}\right) + 1.7 \quad (4)$$

Cooling tower outlet loss coefficient K_{to}

$$K_{to} = -0.28 Fr_D^{-1} + 0.04 Fr_D^{-1.5} \quad (5)$$

$$Fr_D = \left(\frac{M_a}{A_5}\right)^2 / [\rho_{a5}(\rho_{a6} - \rho_{a5}) g d_5 \quad (6)$$

Heat exchanger loss coefficient, K_{he}

$$K_{he} = 31383.9475 Ry^{-0.332458} + \frac{2}{\sigma_a^2}\left(\frac{\rho_{a3} - \rho_{a4}}{\rho_{a3} + \rho_{a4}}\right) \quad (7)$$

In equation 1, $C_{DTs,}$ $L_{ts,}$ n_{ts}, H_3 and ρ_a denotes the drag coefficient of tower, the length of tower support, the number of tower support, the tower inlet height and the air density respectively. In equation 2, σ_c, A_{fr}, and A_{e3} denotes air porosity, frontal area of heat exchanger bundles and effective coverage of area respectively. Also, $Fr_{D,}$ $M_{a,}$ and R_y represents Froude number, air mass flow and Characteristic Reynolds number. The conventional method of heat exchanger is not sufficient for accurate prediction of heat transfer of supercritical fluids. Hence, an iterative nodal approach is adapted where the heat exchanger is sectioned with smaller tube length as if the heat exchangers are connected in series [13]. In nodal approach, the physical property variations with bulk temperature are considered. The traditional log mean temperature difference (LMTD) method is applied at each node. The change of local heat transfer coefficient of sCO_2 with small change of bulk temperature is well predicted by the present technique of iterative nodal approach. In order to evaluate the local convective heat transfer coefficient of sCO_2, Yoon et al. [14] is used.

$$Nu_s = a Re_s^{\,b} Pr_s^{\,c} \left(\frac{\rho_{pc}}{\rho_s}\right)^n \quad (8)$$

a=0.14, b=0.69, c=0.66, n=0 when $T_b > T_{pc}$
a=0.013, b=1.0, c=-0.05, n=1.6 when $T_b \leq T_{pc}$

Here, T_b *and* T_{pc} are the bulk temperature and pseudocritical temperature of the working fluid respectively. The standard package of IPSEpro is used for all the components of the recompression cycle except NDDCT.

NDDCT Performance Analysis

For a 25 MW solar thermal power plant operating with sCO_2 recompression cycle, the required cooling system to accomplish the duty requirements is shown with table 1. The NDDCT is designed for sCO_2 inlet condition of 75^0C, 7.96 MPa, ambient air of 20^0C, cycle pressure ratio of 2.5 and turbine inlet temperature of 650^0C. After designing the required size of NDDCT, next the thermal performance of the tower is carried out at a different ambient temperature from 15^0C to 50^0C.

The figure 7, demonstrates the increase of compressor inlet temperature with the increase of ambient air temperature. The air mass flow rate in the tower linearly decreases with the increase of air temperature. The increased compressor inlet temperature certainly reduces the cycle thermal efficiency, shown in figure 8. The increase of compressor inlet temperature (31.1^0C to 53.1^0C) adversely affects the cycle efficiency. The efficiency drops from 51.1 % to 46.5 % at 50^0C air temperature. The split ratio increases from 60% to 77.7 % with the change of air temperature.

Table 1. NDDCT size for 25 MW solar power plant.

Parameter	Value
Outlet height of tower, H_5	52.45 m
Outlet tower diameter, d_5	26.22 m
Inlet tower diameter, d_3	37.46 m
Number of heat exchanger bundles, n_b	22
Number of tower supports: n_{ts}	26
Length of tower support: lts	6.65 m
Total tube side area	3,924 m^2
sCO_2 mean outlet temperature, T_{so}	34^0C
Air mean outlet temperature, T_{a4}	40.6^0C
Air mass flow rate, M_a	1137 kg/sec

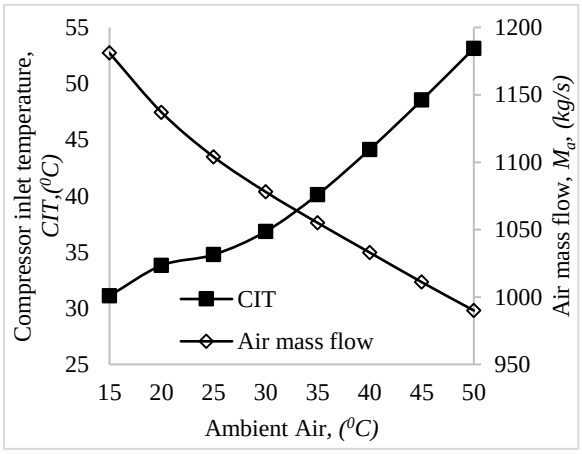

Figure 7. Change of compressor inlet condition and air mass flow in the tower.

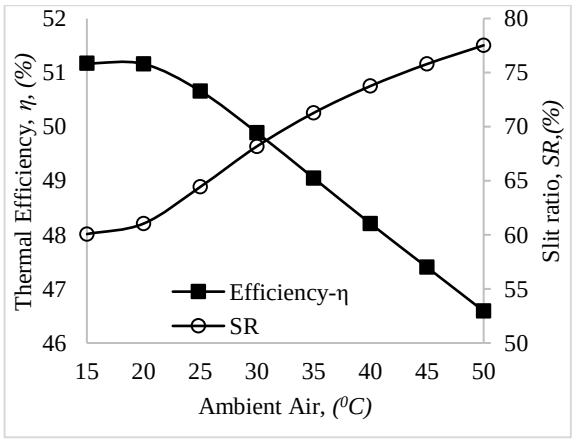

Figure 8. Thermal performance at various ambient air temperature.

Conclusion

In the present work, the required NDDCT size is evaluated for the sCO_2 recompression cycle. The modelling approach takes account of thermodynamic property variations of sCO_2 in the heat exchanger. The preliminary analysis with standard cooler suggests the optimum operating condition, based on which the NDDCT is designed. A dry cooling tower of 52.45 m height and 22 finned tube heat exchanger bundles are required to meet the duty requirements. The cooling performance of NDDCT is significantly affected by the sCO_2 inlet condition and ambient air. During the high-temperature period, the cycle efficiency decreases due to increase of compressor inlet temperature.

Acknowledgment

The first author would also like to acknowledge the University of Queensland (UQ) for providing Research Training Program (RTP) and Australian Postgraduate Award (APA) scholarships. The work is part of a larger project at the UQ towards the development of supercritical CO2 power blocks and cooling system funded by the Australian Renewable Energy Agency (ARENA) under the auspices of Australian Solar Thermal Research Institute (ASTRI).

References

[1] V. Dostal, M. J. Driscoll, P. Hejzlar, and N. E. Todreas, "A supercritical CO2 gas turbine power cycle for next-generation nuclear reactors," *Proc. of ICONE*, vol. 10, p. 2002, 2002.

[2] S. M. Besarati and D. Y. Goswami, "Analysis of advanced supercritical carbon dioxide power cycles with a bottoming cycle for concentrating solar power applications," *Journal of Solar Energy Engineering*, vol. 136, no. 1, p. 010904, 2014.

[3] C. S. Turchi, Z. Ma, T. W. Neises, and M. J. Wagner, "Thermodynamic study of advanced supercritical carbon dioxide power cycles for concentrating solar power systems," *Journal of Solar Energy Engineering*, vol. 135, no. 4, p. 041007, 2013.

[4] T. Conboy, M. Carlson, and G. Rochau, "Dry-Cooled Supercritical CO2 Power for Advanced Nuclear Reactors," *Journal of Engineering for Gas Turbines and Power*, vol. 137, no. 1, p. 012901, 2015.

[5] R. V. Padilla, Y. C. S. Too, R. Benito, and W. Stein, "Exergetic analysis of supercritical CO 2 Brayton cycles integrated with solar central receivers," *Applied Energy*, vol. 148, pp. 348-365, 2015.

[6] R. V. Padilla, Y. C. S. Too, A. Beath, R. McNaughton, and W. Stein, "Effect of pressure drop and reheating on thermal and exergetic performance of supercritical carbon dioxide Brayton cycles integrated with a solar central receiver," *Journal of Solar Energy Engineering*, vol. 137, no. 5, p. 051012, 2015.

[7] C. K. Ho, M. Carlson, P. Garg, and P. Kumar, "Technoeconomic analysis of alternative solarized s-CO2 Brayton cycle configurations," *Journal of Solar Energy Engineering*, vol. 138, no. 5, p. 051008, 2016.

[8] J. D. Osorio, R. Hovsapian, and J. C. Ordonez, "Dynamic analysis of concentrated solar supercritical CO2-based power generation closed-loop cycle," *Applied Thermal Engineering*, vol. 93, pp. 920-934, 2016.

[9] L. Li, Y. Ge, X. Luo, and S. A. Tassou, "Experimental investigation on power generation with low grade waste heat and CO2 transcritical power cycle," *Energy Procedia*, vol. 123, pp. 297-304, 2017.

[10] M. M. Ehsan, Z. Guan, and A. Klimenko, "A comprehensive review on heat transfer and pressure drop characteristics and correlations with supercritical CO2 under heating and cooling applications," *Renewable and Sustainable Energy Reviews*, vol. 92, pp. 658-675, 2018.

[11] M. M. Ehsan, X. Wang, Z. Guan, and A. Klimenko, "Design and performance study of dry cooling system for 25 MW solar power plant operated with supercritical CO2 cycle," *International Journal of Thermal Sciences*, vol. 132, pp. 398-410, 2018.

[12] M. M. Ehsan, Z. Guan, A. Klimenko, and X. Wang, "Design and comparison of direct and indirect cooling system for 25 MW solar power plant operated with supercritical CO2 cycle," *Energy Conversion and Management*, vol. 168, pp. 611-628, 2018.

[13] S. Duniam, I. Jahn, K. Hooman, Y. Lu, and A. Veeraragavan, "Comparison of direct and indirect natural draft dry cooling tower cooling of the sCO2 Brayton cycle for concentrated solar power plants," *Applied Thermal Engineering*, vol. 130, pp. 1070-1080, 2018.

[14] S. H. Yoon, J. H. Kim, Y. W. Hwang, M. S. Kim, K. Min, and Y. Kim, "Heat transfer and pressure drop characteristics during the in-tube cooling process of carbon dioxide in the supercritical region," *International Journal of Refrigeration*, vol. 26, no. 8, pp. 857-864, 2003.